Micropaleontology and Biostratigraphy

Elena Ivanova and Olga Dmitrenko

Abstract To stratify six sediment cores, we applied the calcareous plankton biostratigraphy of the upper sediment cover based on the foraminiferal and nannofossil zonations suggested in Chap. 3 for the Ioffe Drift area. Datum levels (first and last appearances) of zonal index species in individual cores were used to denote zonal boundaries. The oldest recovered sediments are of the Upper Pliocene, probably not older than ~4 Ma. The core correlation suggests a significantly reduced thickness of biostratigraphic zones in the sediment sections from the Ioffe Drift area compared to those in DSDP Site 516 from the neighboring Rio Grande Rise, indicating multiple erosional hiatuses. Moreover, up to five nannofossil and four foraminiferal zones are either washed out or mixed in some cores, supporting the occurrence of hiatuses that result in stratigraphic gaps.

1 Methods

The standard procedure was used to study the down-core species distribution and identify biostratigraphic zones and their boundaries (Ivanova et al. 2016, 2020). The dry sand fractions (>100 μm) from six cores (Table 1) were split to obtain aliquots containing >1000 planktic foraminiferal specimens and then viewed under the STEMI SV6 binocular microscope. These large aliquots were analyzed to better address the species levels of the first (FO) and/or last (LO) occurrence, which could be overlooked in commonly used aliquots of about 300 specimens. This special emphasis was used with species with well-established FO and/or LO datum levels. The sampling interval in the sediment cores varied from 5 to 30 cm, depending on sedimentological features, and it was usually 10 cm. Planktic foraminiferal specimens

E. Ivanova (✉) · O. Dmitrenko
Shirshov Institute of Oceanology, Russian Academy of Sciences, Moscow, Russia
e-mail: e_v_ivanova@ocean.ru

O. Dmitrenko
e-mail: senidol@yandex.ru

I. Murdmaa and E. Ivanova (eds.), *The Ioffe Drift*, Springer Geology,
https://doi.org/10.1007/978-3-030-82871-4_7

Table 1 Accelerator mass-spectrometry (AMS) radiocarbon dates from the Ioffe Drift and Rio Grande Rise. Dates from core AI-3318 after Ivanova et al. (2020). Poz–Poznan Radiocarbon Laboratory

Laboratory code	Core	Depth in core (cm)	Dated material	AMS-^{14}C date (years)
Poz-71478	AI-3318	10–11	Mixed planktic foraminifers	33,140 ± 580*
Poz-71479	AI-3318	20–21	Mixed planktic foraminifers	>46,000*
Poz-71475	AI-3320	5–6	Mixed planktic foraminifers	42,000 ± 2,000
Poz-71476	AI-3320	25–26	Mixed planktic foraminifers	27,350 ± 220
Poz-71467	AI-3321	10–11	Mixed planktic foraminifers	13,420 ± 70
Poz-71468	AI-3321	20–21	Mixed planktic foraminifers	22,050 ± 130

were analyzed from 46 samples in core AI-2436, 55 in core AI-3655, 50 in core AI-3316, 40 in core AI-3317, 34 in core AI-3318 and 30 in core AI-3319. Scanning electron microscope (SEM) photos of several stratigraphically important species were taken on TESCAN VEGA3 and VEGA-II XMU SEMs.

The qualitative abundance of calcareous nannoplankton taxa was established by the examination of smear-slides. Nannofossils were studied from four cores (all apart from AI-3655 and AI-3319) using an Amplival optical microscope (magnification 1,350) and SEM model JSM-U3 (magnification x6,000–10,000). Both microscopes were used for species identification and counting. SEM microphotos with a magnification of x2,000 were taken on TESCAN VEGA3 to identify tiny species. The down-core species distributions were studied in 44 raw samples in core AI-2436, 23 in core AI-3316, 47 in core AI-3317 and 24 in core AI-3318, generally from the same level where planktic foraminiferal specimens were identified.

2 Planktic Foraminiferal Assemblages and Stratigraphic Zones

2.1 Assemblages

Rich warm-water (subtropical to tropical) assemblages occur throughout all six records from the Ioffe Drift area. The upper parts of all cores contain the typical Quaternary species, with a diversity commonly ranging between 20 and 30 taxa per sample, apart from the intervals affected by dissolution. According to the taxonomy developed by Schiebel & Hemleben (2017), the extant species in the material studied

include pink and white specimens of *Globigerinoides ruber* and *Globoturborotalita rubescens, Globigerinoides succucifer, Globorotalita tenella, Globigerinita glutinata, Neogloboquadrina dutertrei, Globorotalia menardii, Globorotalia inflata, Globigerinoides conglobatus, Globigerinella calida, Globigerinella siphonifera, Globoturborotalita tenella, Sphaeroidinella dehiscens*, *Neogloboquadrina incompta, Globorotalia crassaformis, Globorotalia truncatulinoides, Globorotalia hirsuta, Globigerina bulloides, Globigerina falconensis, Pulleniatina obliquiloculata, Orbulina universa,* and other species.

Several extinct Neogene–Quaternary species appeared down-core at various levels, including *Globorotalia crassaformis hessi, Globorotalia crassaformis viola, Globorotalia tosaensis, Globorotalia triangula, Globigerinoides fistulosus, Neogloboquadrina humerosa, Neogloboquadrina acostaensis, Globorotalia exilis, Globorotalia miocenica, Globorotalia multicamerata, Globorotalia margaritae, Pulleniatina primalis, Pulleniatina praecursor, Globigerina decoraperta, Globigerinoides obliquus extremus, Globorotalia pertenuis, Globorotalia limbata, Globorotalia puncticulata, Globorotalia plesiotumida, Dentoglobigerina altispira, Globoquadrina venezuelana, Sphaeroidinellopsis seminulina* and *Sphaeroidinellopsis kochi,* according to the taxonomy developed by Kennett and Srinivasan (1983) and Bolli and Saunders (1985).

SEM images of the most important taxa, including zonal index species, are provided in Plates 1, 2 and 3.

The same extant species were reported in the diverse assemblages of good-to-perfect preservation studied from both a shallow core, AI-3320, and a deeper core, AI-3321, collected respectively from the summit and slope of the Rio Grande Rise (see Table 1 in Chap. 4). In core AI-3320, rather well-preserved aragonite shells of some pteropod species were documented in Levels 0 and 35 cm, including *Styliola subula, Limacina inflata, Limacina bulimoides* and others.

It should be noted that upward microfossil reworking and/or down-core contamination is quite common in all cores studied. These phenomena are known to be typical also of the nearby Rio Grande Rise (Berggren et al. 1983a, b; Barash et al. 1983). Thus, we conclude that these phenomena have to be considered, at least, as regional, and the Ioffe Drift biochronostratigraphy must be developed with caution.

2.2 Foraminiferal Preservation

In all six cores studied from the Ioffe Drift, down-core foraminiferal and calcareous nannofossil preservation generally varies from perfect to moderate; however, several levels are affected by a significant selective dissolution resulting in poor preservation of calcareous microfossils (Figs. 1, 2, 3, 4, 5 and 6). Foraminiferal preservation is generally good to perfect on the drift summit, where weak dissolution was documented only in a few levels (145 cm in core AI-3655; 210–220 cm in core AI-3618; and 109, 207, 225, 350, 430–438, 600, 640–650 and 710 cm in core AI-2436). Dissolution is more common in the deeper cores from the drift slope. In core AI-3316,

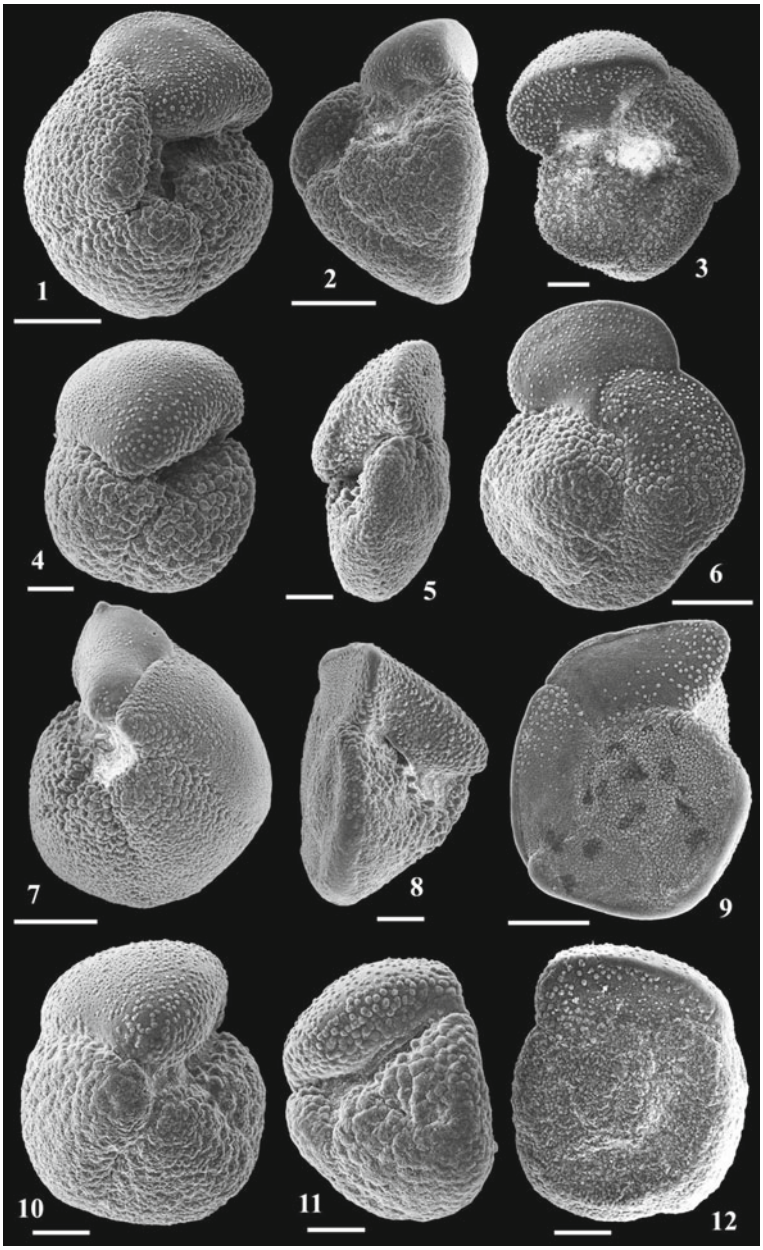

Plate 1 SEM images of planktic foraminiferal species: 1–3. Globorotalia crassaformis hessi, AI-3317, 330 cm, 1, 2 scale bar = 200 μm, 3 scale bar = 100 μm; 4–6. Globorotalia crassaformis viola, AI-3318, 290 cm, 4, 5 scale bar = 100 μm, 6 scale bar = 200 μm; 7–9. Globorotalia truncatulinoides, AI-2436, 286 cm, 7, 9 scale bar = 200 μm, 8 scale bar = 100 μm; 10–12. Globorotalia tosaensis, AI-3318, 210 cm, scale bar = 100 μm

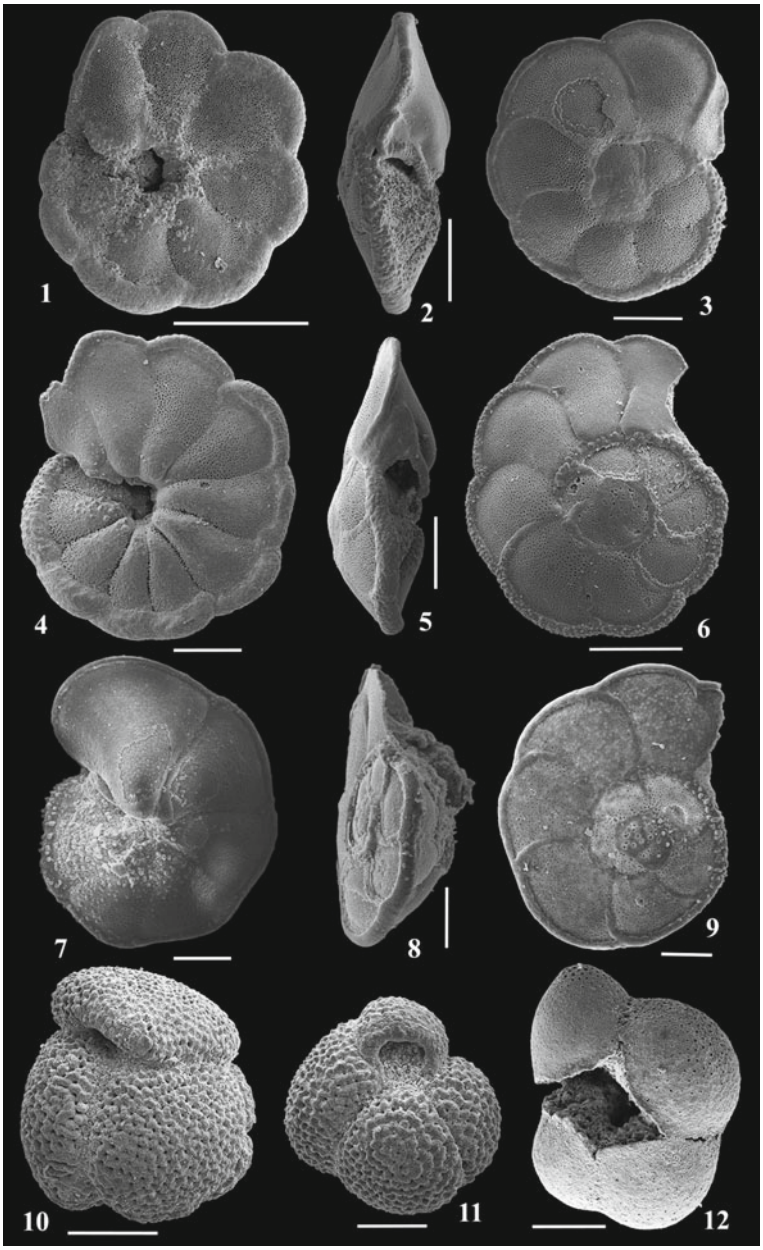

Plate 2 SEM images of planktic foraminiferal species: 1–3. Globorotalia pertenuis, AI-3316, 300 cm, 1 scale bar = 500 μm, 2, 3 scale bar = 200 μm; 4–6. Globorotalia multicamerata, AI-2436, 660 cm, scale bar = 200 μm; 7–9. Globorotalia miocenica, AI-3317, 360 cm, scale bar = 100 μm; 10–11. Globigerinoides obliquus extremus, AI-2436, 660 cm, 10. scale bar = 200 μm, 11 scale bar = 100 μm; 12. Sphaeroidinellopsis kochi, AI-2436, 700 cm, scale bar = 200 μm

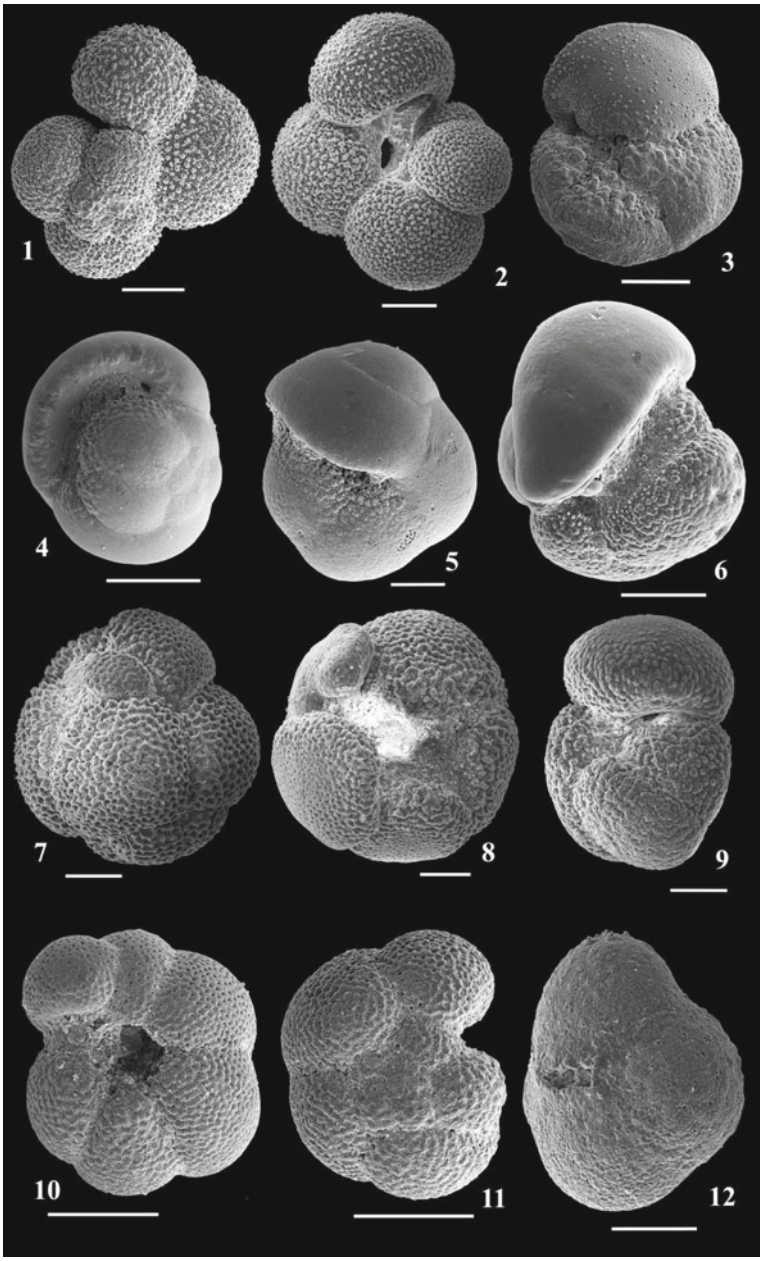

Plate 3 SEM images of planktic foraminiferal species: 1–3. Globigerinella calida calida, AI-3317, 125 cm, 1, 2 scale bar = 100 μm, 3. Globorotalia hirsuta, AI-2436, 400 cm, scale bar = 100 μm; 4. Pulleniatina praecursor, AI-3317, 512 cm, 4. scale bar = 200 μm; 5, 6. Pulleniatina primalis, 5. AI-3316, 420 cm, scale bar = 100 μm, AI-3317, 512 cm, scale bar = 200 μm; 7–9. Dentoglobigerina altispira, AI-3317, 512 cm, scale bar = 100 μm; 10, 11 Neogloboquadrina humerosa, AI-3316, 320 cm, scale bar = 200 μm; 12. Sphaeroidinellopsis seminulina, AI-3317, 512 cm, scale bar = 100 μm

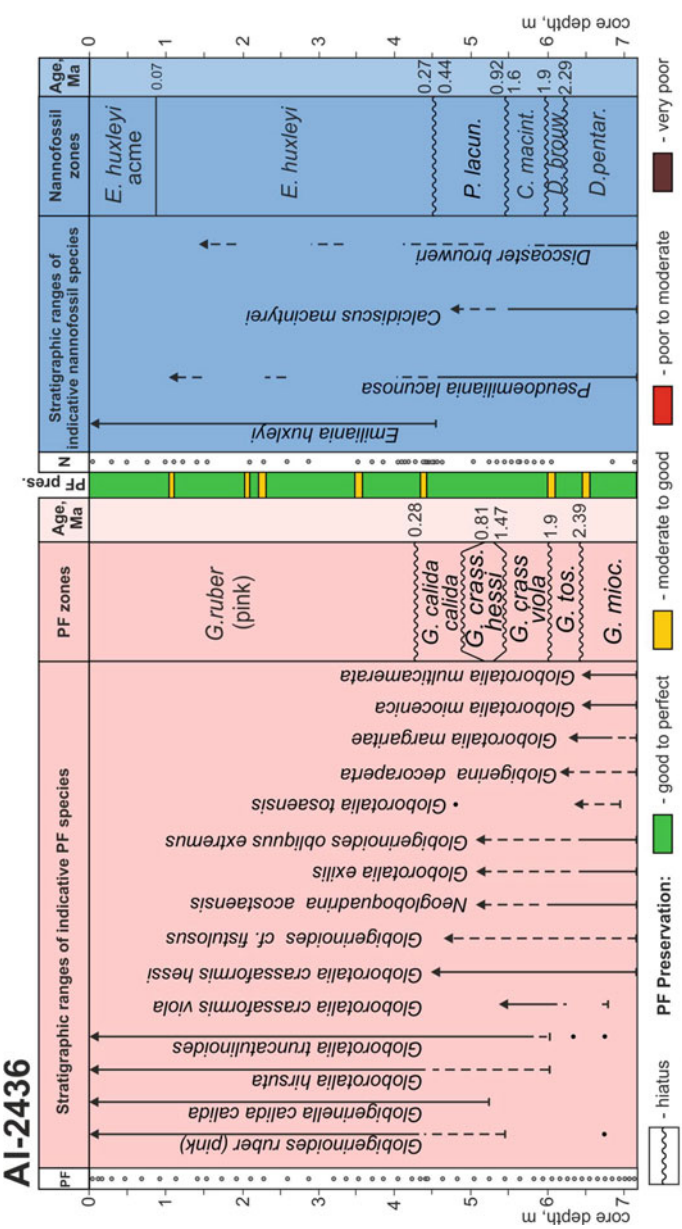

Fig. 1 Stratigraphy of core AI-2436: ranges of indicative species, planktic foraminiferal (PF) and nannofossil zones with their ages (modified from Ivanova et al. 2016). Samples studied for PF and nannofossils (N) are marked by dots in corresponding columns. Arrows indicate the last (presumably in situ) occurrence of species. See text for the species full names

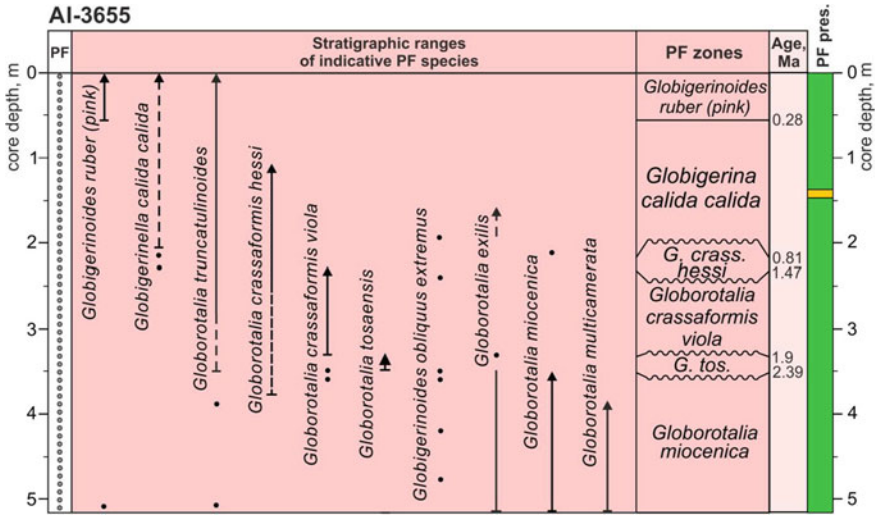

Fig. 2 Stratigraphy of core AI-3655: ranges of indicative species, planktic foraminiferal (PF) zones with their ages and foraminiferal preservation (PF pres.). Samples studied for PF are marked by dots in corresponding column. Arrows indicate the last (presumably in situ) occurrence of species. See text for the species full names and Fig. 1 for legend

good preservation dominates in the upper section and moderate is reported at 27, 47, 137, 147, 187, 257, 277, 307, 347 and 467 cm, while significant dissolution and poor preservation were noted at 377 and 407–427 cm. Similarly, in core AI-3317, significant dissolution was found in the lower part of the section, from 415 to 512 cm, while, upward, preservation was reported commonly as good, with some dissolution documented at a few levels including 25, 145, 155, 385 and 405 cm. In core AI-3319, collected to the WSW of the drift, moderate to heavy dissolution is characteristic of the lower part of the section, from 125 to 291 cm. Weaker dissolution was noted at 75–85 cm, while all other samples demonstrate rather good preservation.

2.3 Planktic Foraminiferal Zones

Despite the medium to poor down-core preservation in some sections, the occurrence of index species allowed the identification of planktic foraminiferal zones in all the cores investigated from the Ioffe Drift area (see Table 1 in Chap. 4). As a result, the foraminiferal zonation described in Chap. 3 (all units are referred to as "zones") was applied to stratify six sediment cores, as follows.

In core **AI-2436** from the drift summit (water depth 3,799 m, Fig. 1; Ivanova et al. 2016), which was collected the first and significantly stretched as a result of core processing (see Chap. 4), the uppermost zone was that of *Globigerinoides ruber* (pink) (430–0 cm, 0.28–0 Ma), with the persistent occurrence of the index species.

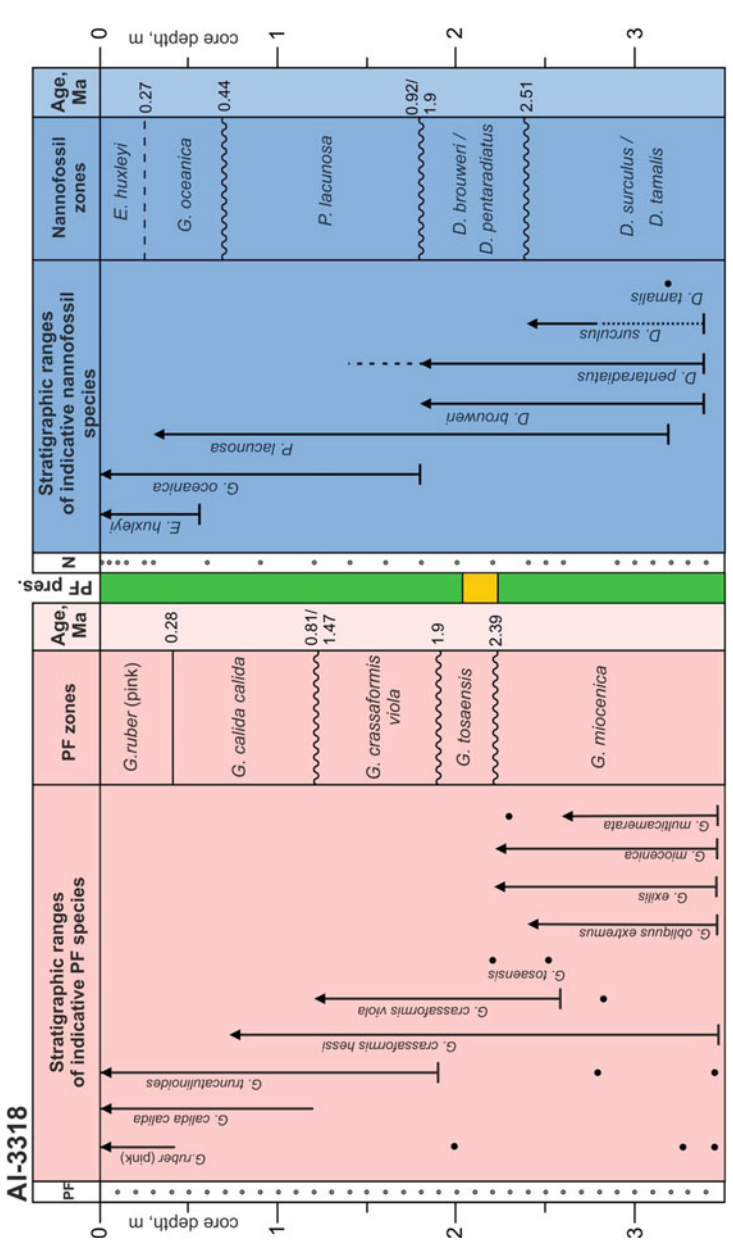

Fig. 3 Stratigraphy of core AI-3318: ranges of indicative species, planktic foraminiferal (PF) and nannofossil zones with their ages (modified from Ivanova et al. 2020) and foraminiferal preservation (PF pres.). Samples studied for PF and nannofossils (N) are marked by dots in corresponding columns. Arrows indicate the last (presumably in situ) occurrence of species. See text for the species full names and Fig. 1 for legend

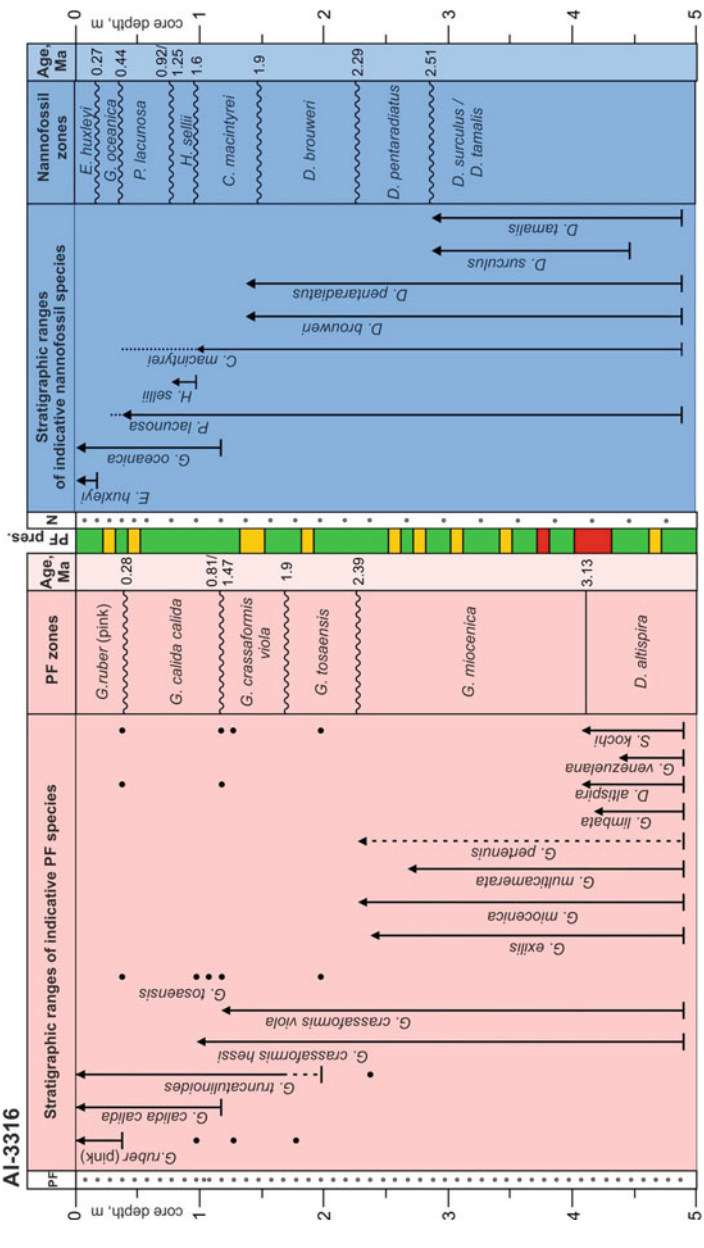

Fig. 4 Stratigraphy of core AI-3316: ranges of indicative species, planktic foraminiferal (PF) and nannofossil zones with their ages (modified from Ivanova et al. 2020) and foraminiferal preservation (PF pres.). Samples studied for PF and nannofossils (N) are marked by dots in corresponding columns. Arrows indicate the last (presumably in situ) occurrence of species. See text for the species full names and Fig. 1 for legend

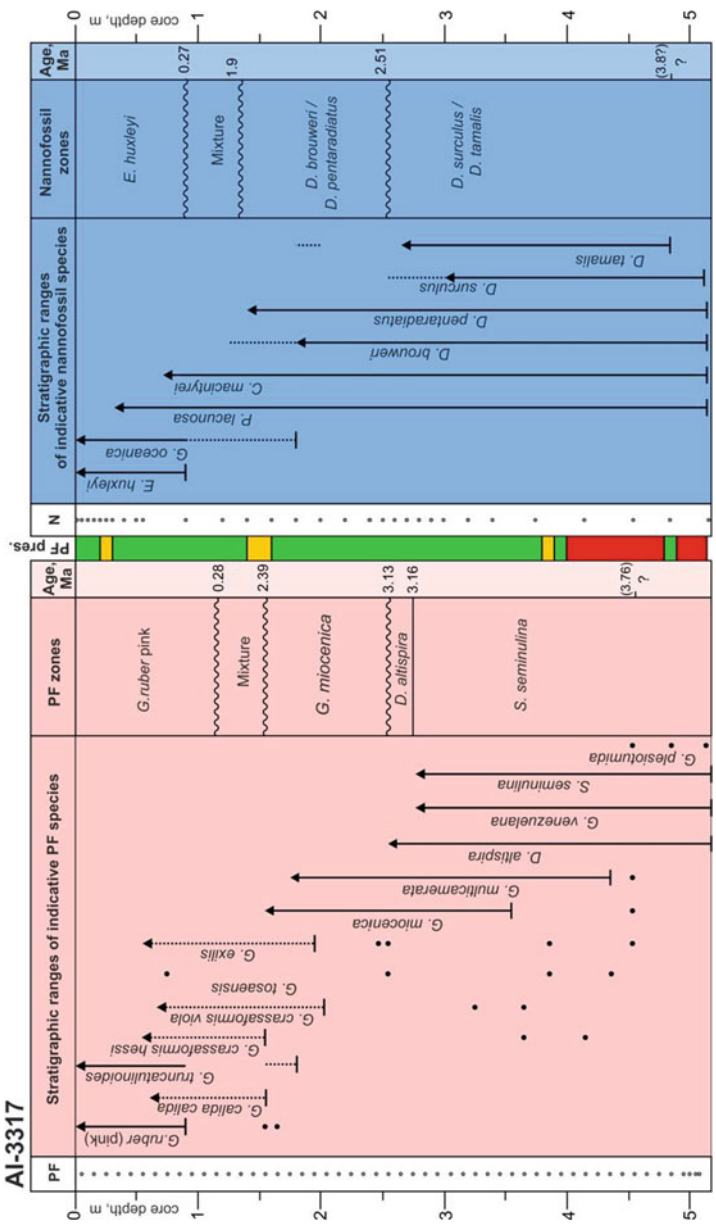

Fig. 5 Stratigraphy of core AI-3317: ranges of indicative species, planktic foraminiferal (PF) and nannofossil zones with their ages and foraminiferal preservation (PF pres.). Samples studied for PF and nannofossils (N) are marked by dots in corresponding columns. Arrows indicate the last (presumably in situ) occurrence of species. See text for the species full names and Fig. 1 for legend

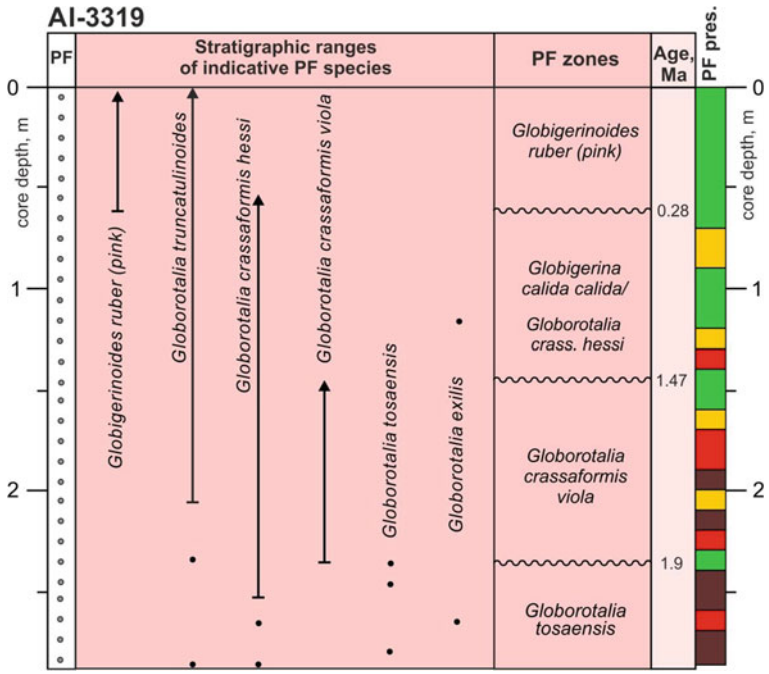

Fig. 6 Stratigraphy of core AI-3319: ranges of indicative species, planktic foraminiferal (PF) zones with their ages and foraminiferal preservation (PF pres.). Samples studied for PF are marked by dots in corresponding column. Arrows indicate the last (presumably in situ) occurrence of species. See text for the species full names and Fig. 1 for legend

Globigerinella calida calida zone (0.81–0.28 Ma) was identified within the interval 520–430 cm, based on the occurrence of the nominate taxon as well as *Globorotalia crassaformis hessi* and *G. truncatulinoides.* The lower boundary of the underlying rudimentary zone of *Globorotalia crassaformis hessi* (530–520 cm, 1.47–0.81 Ma) is marked by the LO of *Globorotalia crassaformis viola,* an indicative species of the underlying same-named zone (600–530 cm, 1.9–1.47 Ma). The upper boundary of an also reduced underlying zone of *Globorotalia tosaensis* (640–600 cm) was defined by the FO of *G. truncatulinoides* at ~1.9 Ma. The latter species occurs persistently within the upper 600 cm of the core, whereas *G. tosaensis* occurs randomly at a few levels.

The boundary between zones of *Globorotalia tosaensis* and *Globorotalia miocenica* were inferred from the disappearance of Neogene species including *Globorotalia multicamerata* and *G. miocenica* at 640 cm. As mentioned in Chap. 3, the latter datum level was adopted from Wade et al. (2011), namely the LO of *G. miocenica* at about 2.39 Ma. Although the LO of *G. multicamerata* is suggested to be older, ~3 Ma (Wade et al. 2011, see Chap. 3), in core AI-2436 both species disappeared simultaneously, probably due to the strongly reduced thickness of the stratigraphic zones. The lowermost part of the core (714–640 cm) is referred to as the

recovered part of *Globorotalia miocenica* zone on the basis of the occurrence of nominate taxon, *Globigerina decoraperta, Sphaeroidinellopsis seminulina, Globorotalia exilis, Globigerinoides obliquus extremus, Neogloboquadrina acostaensis, Globorotalia multicamerata* and *Globigerinoides fistulosus.* The assumption about the Upper Pliocene character of foraminiferal fauna is corroborated by the absence of older Pliocene species, such as *Globoquadrina dehiscens* and *Dentoglobigerina altispira*, and of the above-mentioned indicative Pleistocene species. The reduced thickness of foraminiferal zones in the core section indicates the occurrence of several hiatuses, especially pronounced in *Globorotalia crassaformis hessi* zone.

Another core, AI-3655, was collected from the drift summit (water depth 3,799 m) in order to overcome the problems for the stratigraphy caused by core AI-2436 stretching. Core **AI-3655** recovered the same foraminiferal zones, according to the down-core distributions of the nominate taxa (Fig. 2). The *Globigerinoides ruber* (pink) zone is only 58 cm thick (as it was not stretched), whereas the underlying zone of *Globigerinella calida calida* (218–58 cm) is considerably thicker than in core AI-2436; however, its lower boundary is doubtful, like that of the underlying *Globorotalia crassaformis hessi* zone (230–218 cm). These two are challenging to identify in both cores due to the rare occurrence of a species susceptible to dissolution: *G. calida calida.* Therefore, the boundary of the *Globorotalia crassaformis hessi* and *Globorotalia crassaformis viola* zones (330–230 cm), and the thickness of the latter, are questionable. The *Globorotalia tosaensis* zone (350–330 cm) is strongly reduced, whereas the lowermost recovered zone of *Globorotalia miocenica* (514–350 cm) is rather well represented in core AI–3655. Several hiatuses in the core section are suggested by the reduced thickness of most foraminiferal zones.

In core **AI-3318** from the drift summit (water depth 3,788 m, Ivanova et al., 2020), pink specimens of *Globigerinoides ruber* occur continuously in the upper 40 cm, defining the self-titled uppermost foraminiferal zone (Fig. 3). The absence of Holocene sediments and the Late Pleistocene age of the upper 20 cm of the core section were ascertained by two AMS-^{14}C dates of 33,140 ± 580 ka and >46,000 ka BP, obtained at 10 and 20 cm, respectively (Table 1). Scarce tests of *G. ruber* were found at 192, 326 cm and in the core-catcher (CC), probably as a result of core processing and/or down-core contamination. Based on the down-core distribution of index species, the zone of *Globigerinella calida calida* (0.81–0.28 Ma) is tentatively identified as between 120 and 40 cm, while *Globorotalia crassaformis hessi* zone (1.47–0. 81 Ma) is probably washed out, suggesting a hiatus at 120 cm, where both the FO of *G. calida calida* and the LO of *G. viola* were reported at the same level. The base of the underlying *Globorotalia crassaformis viola* zone (1.9–1.47 Ma) is defined by the persistent occurrence of *G. truncatulinoides* above 190 cm. The *Globorotalia tosaensis* zone (2.39–1.9 Ma) bounded below by the LO of *Globorotalia miocenica* covering the interval 220–190 cm, possibly with both lower and upper boundaries represented by hiatuses in line with the comparison with magnetic susceptibility data (see Chapter 9). Some extinct Pliocene species notably *Globorotalia exilis, G. multicamerata* and *Globigerinoides obliquus extremus,* disappear in *Globorotalia miocenica* zone (340–220 cm) or PL5 (after Berggren et al. 1995). Single specimens

of *Globorotalia pertenuis, G. margaritae* and other extinct species were also documented in this zone. The *Globorotalia miocenica* zone seems not to be completely recovered, as the LO of *Dentoglobigerina altispira* (3.13 Ma, according to Wade et al. 2011) is not identified.

The same and some older extinct taxa are found in core **AI-3316** from the northern slope of the drift, which penetrated stratigraphically deeper than the three cores from the drift summit (water depth 3,898 m, Ivanova et al. 2020). In the core section, foraminiferal zones are defined according to the nominate taxa distribution, as follows: *Globigerinoides ruber* (pink) from 37 to 0 cm, *Globigerinella calida calida* from 117 to 37 cm, *Globorotalia crassaformis viola* from 167–117 cm and *Globorotalia tosaensis* from 227 to 167 cm (Fig. 4). The *Globorotalia crassaformis hessi* zone is not preserved in the core section and a hiatus is assumed at 117 cm. The *Globorotalia tosaensis* zone seems also to be bounded by hiatuses (see Chap. 9). The *Globorotalia miocenica* (or PL5) zone is documented between the LO of the same named species and the LO of *Dentoglobigerina altispira,* at 227 cm and 407 cm, respectively. The lowermost *Dentoglobigerina altispira* zone (or PL4, 3.16–3.13 Ma, 489–407 cm) contains common specimens of Neogene species along with index species, notably *Globorotalia limbata, Globoquadrina venezuelana* and *Sphaeroidinellopsis kochi*. According to Kennett and Srinivasan (1983), the latter two species are typical of the tropical early Pliocene zone N19, after Blow (1969). They were probably reworked upward. A significant dissolution of foraminiferal shells was reported from two intervals of the lowermost zones of *Globorotalia miocenica* and *Dentoglobigerina altispira.*

The most stratigraphically biased core **AI-3317** from the northern slope (water depth 3,832 m) probably penetrated deeper into the Pliocene section than any other core. It is characterized by rather significant contamination and reworking, which are probably stronger than elsewhere. The uppermost *Globigerinoides ruber* (pink) zone is identified from 115 to 0 cm by the persistent occurrence of the zonal marker (Fig. 5); however, the underlying 40 cm interval contains a mixture of several index species and probably overlies a hiatus. The sediments of the *Globigerinella calida calida, Globorotalia crassaformis hessi, Globorotalia crassaformis viola* and *Globorotalia tosaensis* zones are washed out by bottom-water erosion, with only mixed remnants in the 155–115 cm interval. The concurrent presence of the above-mentioned taxa suggests some hiatuses within this interval. By contrast, the underlying zones of *Globorotalia miocenica* (255–155 cm) and *Dentoglobigerina altispira* (275–255 cm), respectively PL5 and PL4 (after Berggren et al. 1995), are well documented. Nevertheless, the occurrence of hiatuses cannot be denied within these zones and at their boundaries, especially considering the magnetic susceptibility data (see Chaps. 6 and 9). The *Sphaeroidinellopsis seminulina* zone or PL3 (3.84–3.16 Ma, after Wade et al. 2011) was reported below, within the interval from 255 cm down to at least 455 cm, according to the occurrence and the LO of the nominate taxon. The LO of *Globorotalia plesiotumida* (3.76 Ma, according to Wade et al. 2011) is suggested at 455 cm. The lower part of the zone is characterized by poor foraminiferal preservation due to significant dissolution at several levels.

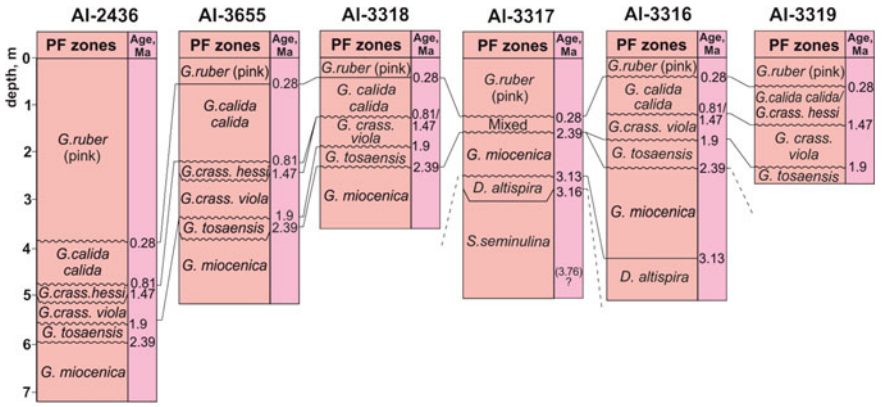

Fig. 7 Correlation of planktic foraminiferal zones in six cores studied. See text for the species full names and Fig. 1 for legend

The deepest and shortest core, **AI-3319,** collected to the WSW of the Ioffe Drift from a water depth of 4,066 m, did not recover the Pliocene/Pleistocene boundary (Fig. 6). Foraminiferal fauna from the lower part of the core, below 170 cm, were heavily affected by dissolution therefore some samples contain only a few whole foraminiferal tests. Nonetheless, the resistance to dissolution of some species, notably globorotaliids, allows the definition of the zones and their boundaries. The *Globigerinoides ruber* (pink) zone, with persistent occurrence of the nominate taxon, was identified from 60 to 0 cm. It is underlined by a combined zone of *Globigerinella calida calida/Globorotalia crassaformis hessi*, probably below a hiatus at ~60 cm. A better-represented *Globorotalia crassaformis viola* zone seems to be bounded by hiatuses at 140 and 235 cm. The lowermost *Globorotalia tosaensis* zone was recovered at an interval of 288–235 cm, demonstrating a visible thickness of 53 cm.

The stratigraphic correlation of foraminiferal zones in the six cores studied from the Ioffe Drift is shown in Fig. 7. This figure documents the best representation of Pleistocene zones in cores AI-2436 and AI-3655, from the drift summit. By contrast, cores AI-3316 and AI-3317 from the northern slope recovered the older sediments of the Upper Pliocene (>3.13 Ma and ~4 Ma, respectively). Correspondingly, the stratigraphically oldest sediments of the *Sphaeroidinellopsis seminulina* zone were recovered only by core AI-3317. In four cores, the *Globigerinella calida calida* and *Globorotalia crassaformis hessi* zones are missing or cannot be properly determined, and are therefore combined. At the same time, core AI-3317 contains a condensed interval of mixed faunal zones, demonstrating the strongest contamination, reworking and erosion.

3 Nannofossil Assemblages and Stratigraphic Zones

In the four cores from the Ioffe Drift (Table 1 in Chap. 4) in which nannofossils were studied, they were common and represented by about 40 taxa. Nannofossil zones were recognized from four cores and the data for three of them were published earlier (Ivanova et al. 2016, 2020). It should be mentioned that the distribution of several index species, for instance small *Gephyrocapsa* (mostly *G. sinuosa* and *G. aperta*), appeared to have been strongly affected by dissolution in corresponding intervals. SEM images of the most important taxa, including zonal index species, are provided in Plates 4, 5, 6, 7 and 8. Here, we applied nannofossil zonation, using the revised dates for the zonal boundaries, as described in Chap. 3 for four cores.

In core **AI-2436** (Fig. 1; Ivanova et al. 2016), from the drift summit, the following Pliocene–Quaternary nannofossil zones were inferred downcore: *Emiliania huxleyi* zone, 452–0 cm (0.27–0 Ma), including the *E. huxleyi* Acme zone at 87–0 cm (0.07–0 Ma); *Gephyrocapsa oceanica* zone (0.44–0.27 Ma) is probably washed out and has been partly reworked upward; while the interval 548–452 cm delineates *Pseudoemiliania lacunosa* zone (0.92–0.44 Ma). The small *Gephyrocapsa* zone (1.25–0.92 Ma) was not found, while the *Helicosphaera sellii* zone (1.6–1.25 Ma) was probably washed out and its index species reworked into the *E. huxleyi* zone. The zone of *Calcidiscus macintyrei* (1.9–1.6 Ma) is defined by the interval 595–548 cm, above the persistent occurrence of *Discoasters*. The lowermost part of the core (714–595 cm) consists of two zones: a rudimentary *Discoaster brouweri* zone (620–595 cm, 2.29–1.9 Ma); and a recovered part of zone *Discoaster pentaradiatus* (714–620 cm). The absence of some zones and the rudimentary character of the others clearly point to hiatuses, at least at 452 cm (0.44/0.27 Ma), 548 cm (1.51/0.92 Ma), 595 cm (1.9 Ma) and 620 cm (2.29 Ma).

In core **AI-3318** (Figs. 3 and 8; Ivanova et al. 2020) from the drift summit, *Emiliania huxleyi* occurs in the upper 55 cm and its upward-increasing abundance defines the lower boundary (0.27 Ma) of the uppermost self-titled zone, presumably at 25 cm. Other index species, *Gephyrocapsa oceanica* and *Pseudoemiliania lacunosa,* were reported from the intervals 180–0 cm and 340–25 cm, respectively. The boundary between the zones of these names at 0.44 Ma is tentatively located at 70 cm on the basis of the increasing abundance of *G. oceanica* and decreasing abundance of *P. lacunosa,* and the hiatus is very likely to have occurred at this level. The lower boundary of the *Pseudoemiliania lacunosa* zone (0.92 Ma), represented by a hiatus, is tentatively placed at 180 cm, whereas the three underlying zones of Gartner's scheme (1977), notably the zones of small *Gephyrocapsa* (1.25–0.92 Ma), *Helicosphaera sellii* (1.6–1.25 Ma) and *Calcidiscus macintyrei* (1.9–1.6 Ma), seem to have been washed out. Various *Discoasters* occur persistently down-core below 180 cm, while specimens of *D. pentaradiatus* are probably contaminated upwards to 140 cm. The existing limits to resolution allow no greater refinement than the combined zones of *Discoaster brouweri/Discoaster pentaradiatus* (2.51–1.9 Ma) and of *Discoaster surculus/Discoaster tamalis* (2.51–2.73 Ma) within the intervals of 240–180 cm and 345–240 cm, respectively. The LO of *D. surculus* defines the boundary between

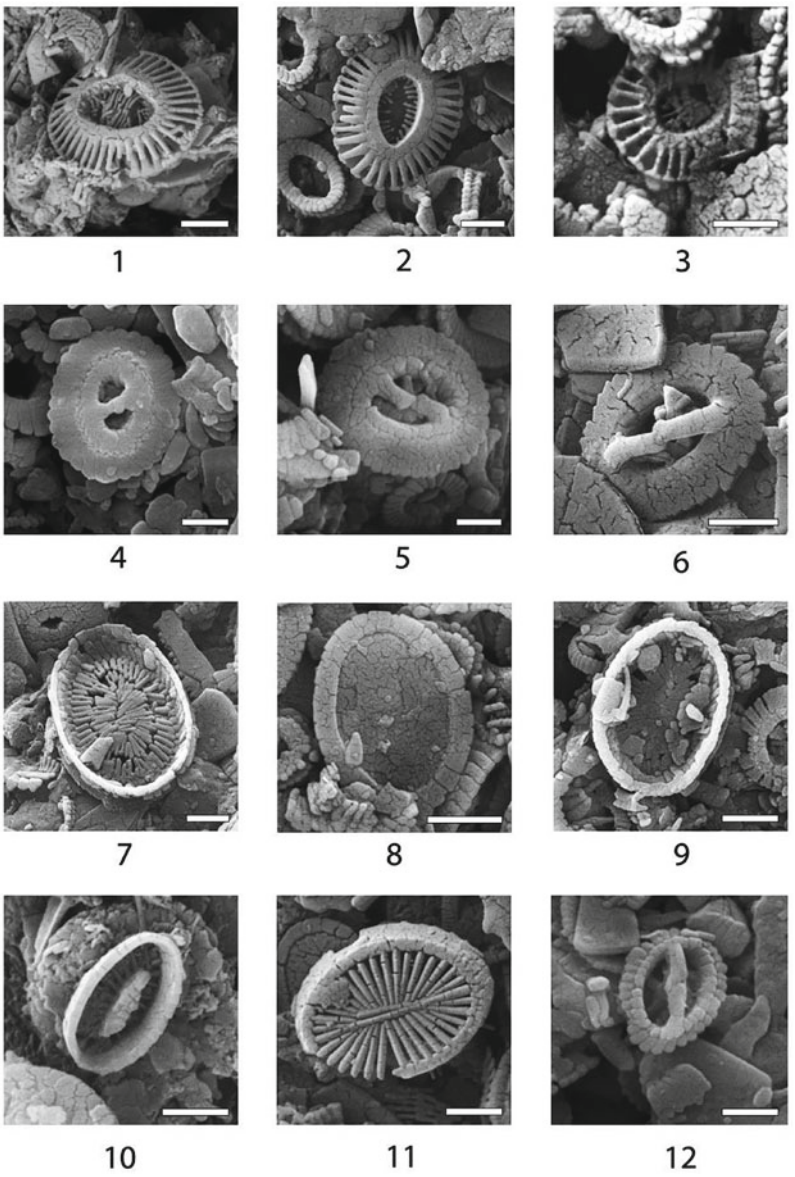

Plate 4 SEM images of nannofossils from Core AI–3318: 1–3. Emiliania huxleyi (Lohm.) Hay, Mohl., scale bar = 1 μm; 1–55, 2–20, 3–180 cm. 4. Gephyrocapsa oceanica Kpt., 280 cm, scale bar = 1 μm. 5,6. Gephyrocapsa caribbeanica Boudr., Hay, scale bar = 1 μm; 5–340, 6–0 cm. 7, 9. Syracosphaera pulchra Lohm., 7–15 cm, scale bar = 1 μm, 9–300 cm, scale bar = 2 μm. 8. Syracosphaera cf. pulchra Lohm., 290 cm, scale bar = 2 μm. 10. Syracosphaera ossa (L.-Schl.) Loedl., Tapp., scale bar = 1 μm. 11. Syracosphaera sp., scale bar = 1 μm. 12. Gephyrocapsa aperta Kpt., 50 cm, scale bar = 1 μm

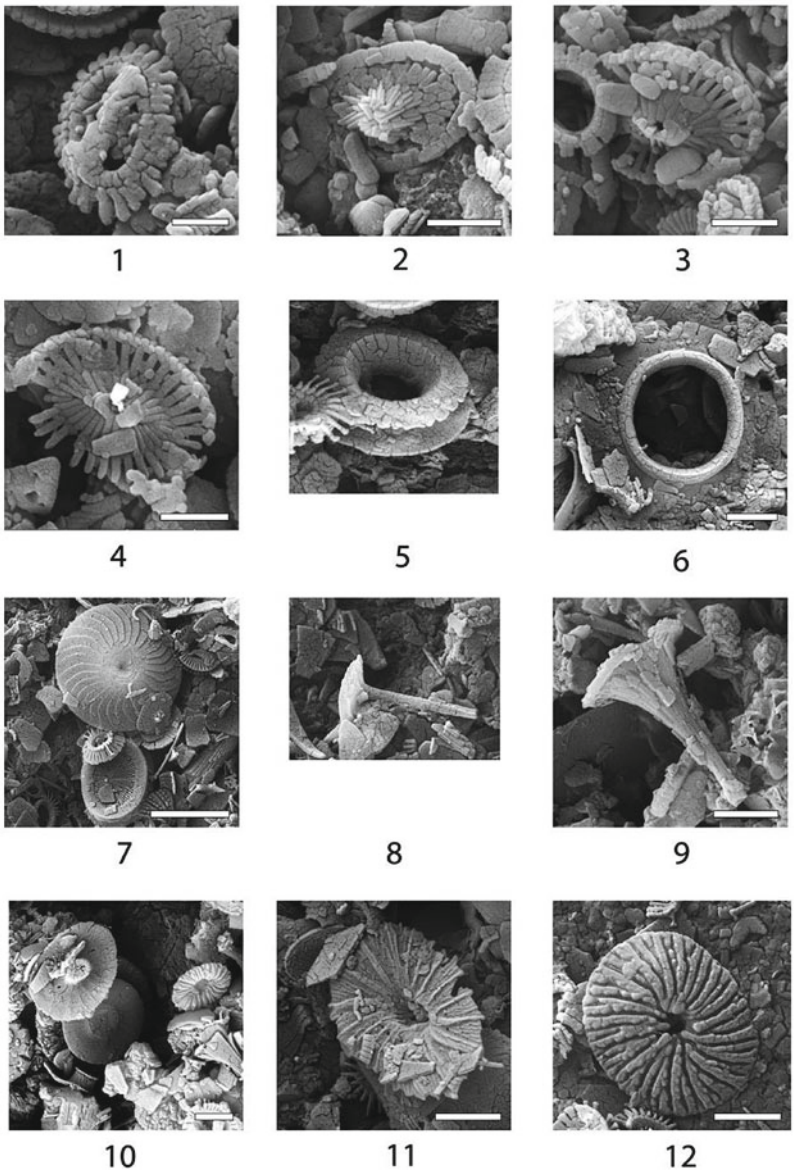

Plate 5 SEM images of nannofossils from Core AI–3318: Core AI–3318. 1. Gephyrocapsa protohuxleyi McIntyrei, 50 cm, scale bar = 1 μm. 2–4. Acanthoica quattrospina Lohm., scale bar = 2 μm. 2, 3–280 cm. 4–300 cm. 5. Umbilicosphaera sibogae (Weber van Bosse) Gaarder., 10 cm. 6. U. anulus (Lecal) Young, Geisen, 15 cm, scale bar = 2 μm. 7. Calcidiscus leptoporus (Murr., Blackm.) Loebl., 0 cm, scale bar = 5 μm. 8. Discosphaera tubifera (Murr., Blackm.) Kpt., 0 cm. 9, 10. Umbellosphaera irregularis Paasche; 55 cm, scale bar = 2 μm. 11, 12. Umbellosphaera tenuis (Kpt.) Paasche, scale bar = 2 μm; 11–5, 12–0 cm

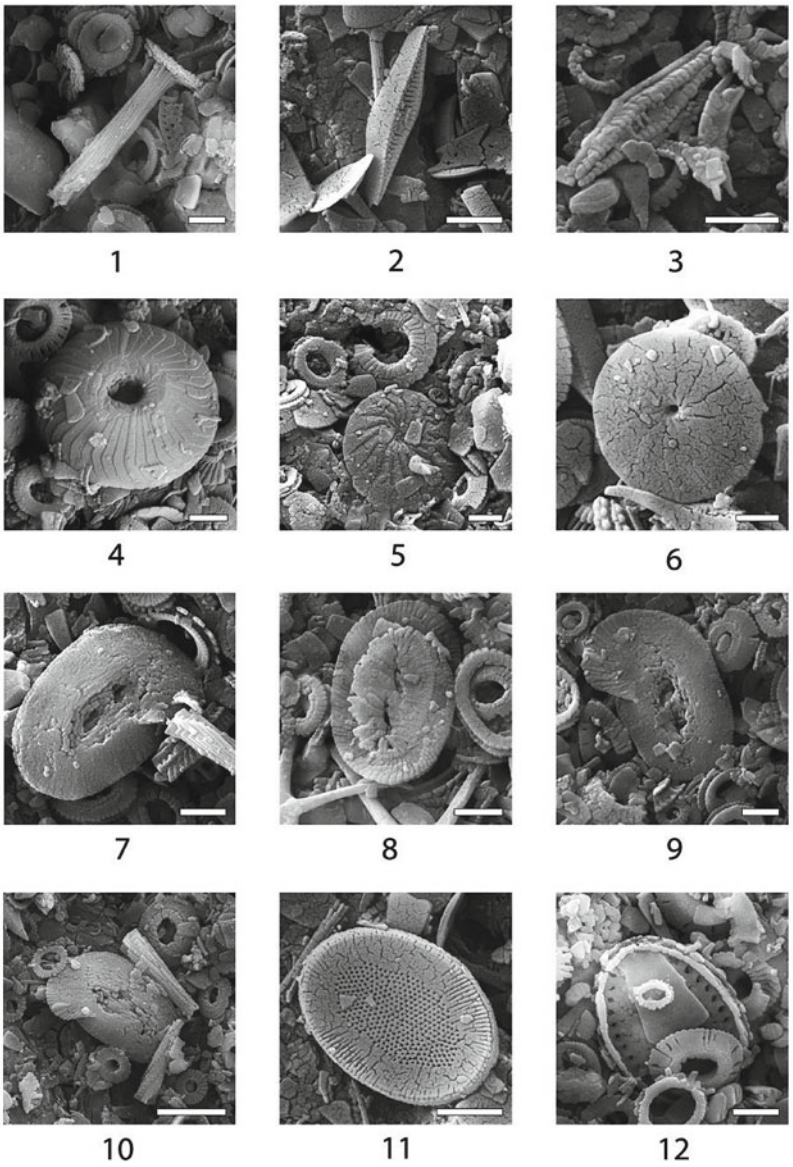

Plate 6 SEM images of nannofossils from the Ioffe Drift sections: 1. Rhabdosphaera clavigera (Murr., Blackm.) Kpt., 140 cm, scale bar = 2 μm. 2, 3. Scapholithus fossilis Defl., scale bar = 2 μm, 2–0, 3–120 cm. 4. Calcidiscus macintyrei (Bukry, Bram.) Loebl., Tapp., 160 cm, scale bar = 2 μm. 5, 6. Oolithothus antillarum (Cohen) Rein, 5–25 cm, scale bar = 2 μm, 6–160 cm, scale bar = 1 μm. 7. Helicosphaera carteri (Wall.) Kpt., 90 cm, scale bar = 2 μm. 8. Helicosphaera wallichii (Lohm.) Boudr., Hay, 55 cm, scale bar = 2 μm. 9. Helicosphaera sellii Bukry, Bram., 260 cm, scale bar = 2 μm. 10. Helicosphaera hyalina Gaarder, 60 cm, scale bar = 5 μm. 11. Pontosphaera japonica (Tak.) Nish. 0 cm, scale bar = 2 μm. 12. Pontosphaera multipora (Kpt.) Roth., 140 cm, scale bar = 2 μm

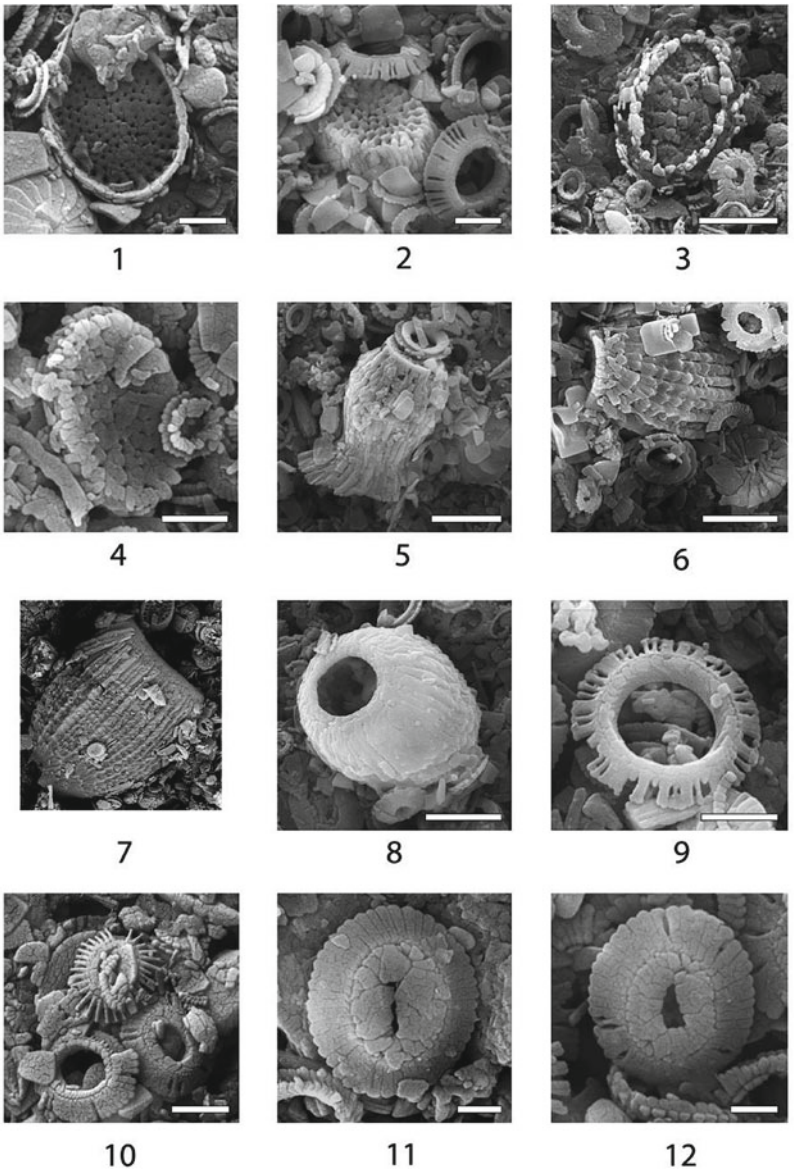

Plate 7 SEM images of nannofossils from Core AI–3318: 1, 2. Pontosphaera multipora (Kpt.) Roth., scale bar = 2 μm, 1–140 cm, 2– 45 cm. 3, 4. Pontosphaera segmenta (Bukry, Perciv.), 3–45 cm, scale bar = 5 μm, 4–340 cm, scale bar = 2 μm. 5. Scyphosphaera amphora Defl., 220 cm, scale bar = 5 μm. 6, 7. Scyphosphaera aranta Kpt.; 6–310 cm, scale bar = 5 μm, 7–60 cm. 8. Scyphosphaera globulata Bukry, Perciv, 45 cm, scale bar = 5 μm. 9, 10. Pseudoemiliania lacunosa (Kpt.) Gart.; scale bar = 2 μm, 9–140, 10–180 cm. 11, 12. Reticulofenestra pseudoumbilica (Gart) Gart., 11, 12–210 cm, scale bar = 1 μm

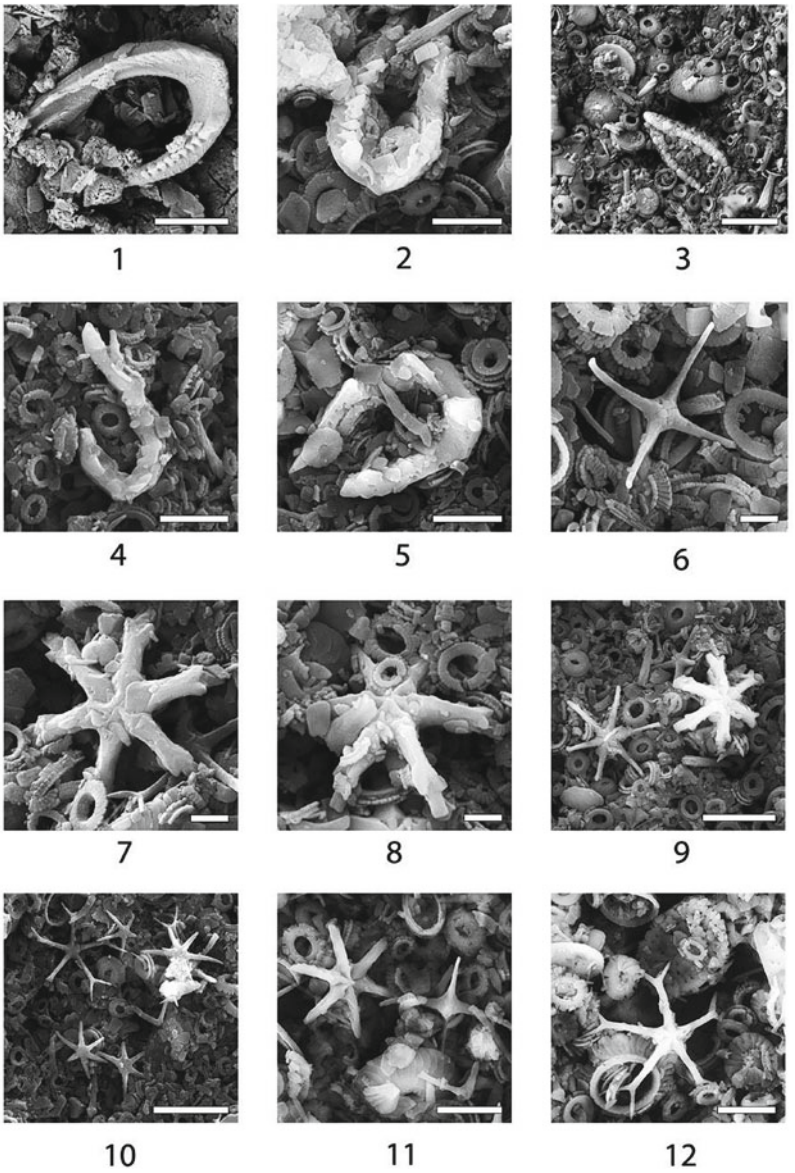

Plate 8 SEM images of nannofossils from the Ioffe Drift sections: Core AI–3318:1. Ceratolithus cristatus Kpt., 55 cm, scale bar = 5 μm. 2,3. Ceratolithus tricorniculatus Gart., 2–90 cm, scale bar = 5 μm, 3–250 cm, scale bar = 10 μm. 4. Ceratolithus acutus Gart., Bukry, 250 cm, scale bar = 5 μm. 5. Ceratolithus rugosus Bukry, Bram., 300 cm, scale bar = 5 μm. 6. Discoaster tamalis Kpt., 310 cm, scale bar = 2 μm. 7–9. Discoaster surculus Mart., Bram; 7–300 cm, scale bar = 2 μm, 8–280 cm, scale bar = 2 μm, 9–290 cm, scale bar = 10 μm, 9 (left) Discoaster calcaris Gart., 10. Discoaster moorei Bukry and Discoaster calcaris Gart., 250 cm, scale bar = 10 μm. Core AI–3316: 11 (left) Discoaster brouweri Tan., (right) Discoaster tamalis Kpt., 197 cm, scale bar = 5 μm. 12. Discoaster pentaradiatus Tan., 267 cm, scale bar = 5 μm

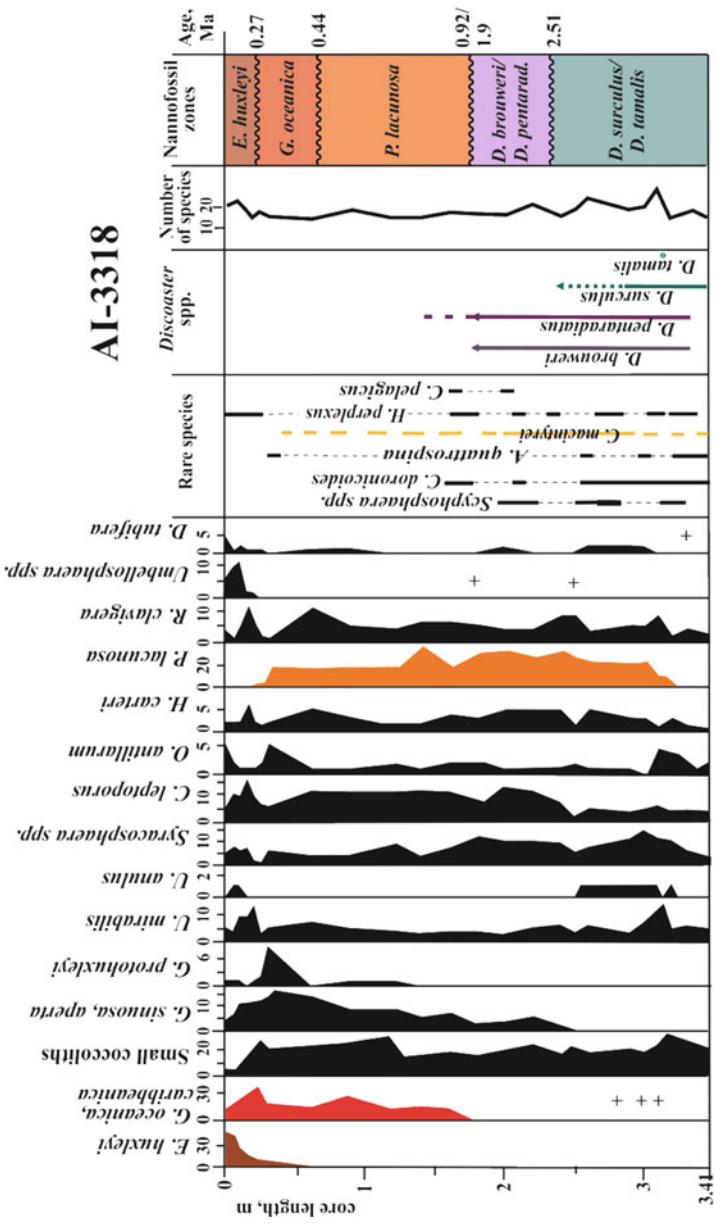

Fig. 8 Down-core distribution of species and nannofossil zones from core AI-3318. See text for the species full names and Fig. 1 for legend

these zones at 240 cm. *D. tamalis* was found in only one sample, from 320 cm. All zonal boundaries in the core, perhaps excepting the uppermost (0.27 Ma), seem to be represented by hiatuses (see also Chap. 9).

In core **AI-3316** (Figs. 4 and 9; Ivanova et al. 2020), from the northern slope of the drift, the presence of *Emiliania huxleyi* in one sample from 7 cm gives the lower erosional boundary of the reduced zone of this same name. Similarly, the other Quaternary zones are strongly reduced, as follows, from the down-core distribution of the zonal markers *Gephyrocapsa oceanica* and *Pseudoemiliania lacunosa* within the intervals 177–7 cm and 489–27 cm, respectively. The boundary between the same-named zones (0.44 Ma) is defined by the last persistent occurrence of the latter species at 37 cm and definitely represents a hiatus. The latter is also true for the boundary between the *Pseudoemiliania lacunosa* (0.92–0.44 Ma) and *Helicosphaera sellii* (1.6–1.25 Ma) zones, at 77 cm, as the small *Gephyrocapsa* zone (1.25–0.92 Ma) is washed out. An interval 97–77 cm, marked by the presence of *H. sellii,* delineates the zone of this name. Although the nominate taxon of the underlying zone *Calcidiscus macintyrei* (1.9–1.6 Ma) occurs up to 37 cm, large coccoliths of the taxa were documented only within the interval 488–97 cm, thereby assigning the boundary of zones *Helicosphaera sellii* and *Calcidiscus macintyrei* to 97 cm. The disappearance of *Discoasters* determines the boundary of the latter zone and the *Discoaster brouweri* zone at 137 cm. Both *D. brouweri* and *D. pentaradiatus* occur downcore below this level; however, the boundary between the same-named zones (2.29 Ma, according to Bergen et al. 2019) could be identified by an upward increase in the latter species abundance up to 227 cm. By contrast, only the combined *Discoaster surculus/Discoaster tamalis* zone (>2.73–2.51 Ma) could be defined in the lower part of the section, from 489 to 287 cm, based on the species distribution within the intervals 448–297 cm and 489–297 cm, respectively. The rather persistent occurrence of *D. tamalis* in the latter interval, together with the absence of *D. surculus* from its lowermost part, suggests that the core recovered at least 2.73 Ma, according to available publications on the datum levels of these species (i.e., Rahman & Rothe, 1989; Backman et al., 2012; Bergen et al., 2019). All zonal boundaries in the core are probably represented by hiatuses (see also Chap. 9).

In the most biased core, **AI-3317**, from the northern slope of the Ioffe Drift (Figs. 5 and 10), the *Emiliania huxleyi* zone is defined as the interval with the persistent occurrence of nominate taxon, at 90–0 cm, while the underlying interval (137–90 cm) contains a mixture of several species and cannot be attributed to any specific nannofossil zone. It is separated by hiatuses from the overlying zone of *E. huxleyi* and the underlying combined zone of *Discoaster brouweri/Discoaster pentaradiatus.* Along with both index species, the latter zone contains specimens of *D. tamalis,* probably reworked from the underlying combined zone of *Discoaster surculus/Discoaster tamalis.* As this species is not found below 485 cm, we assume that the core recovered more than 3.82 Ma (corresponding to the species FO, after Backman et al. 2012).

The correlation of nannofossil zones in the four cores studied from the Ioffe Drift (Fig. 11) demonstrates that they are better represented in core AI-3316, from northern slope of the drift than in the other three cores. In the drift summit cores

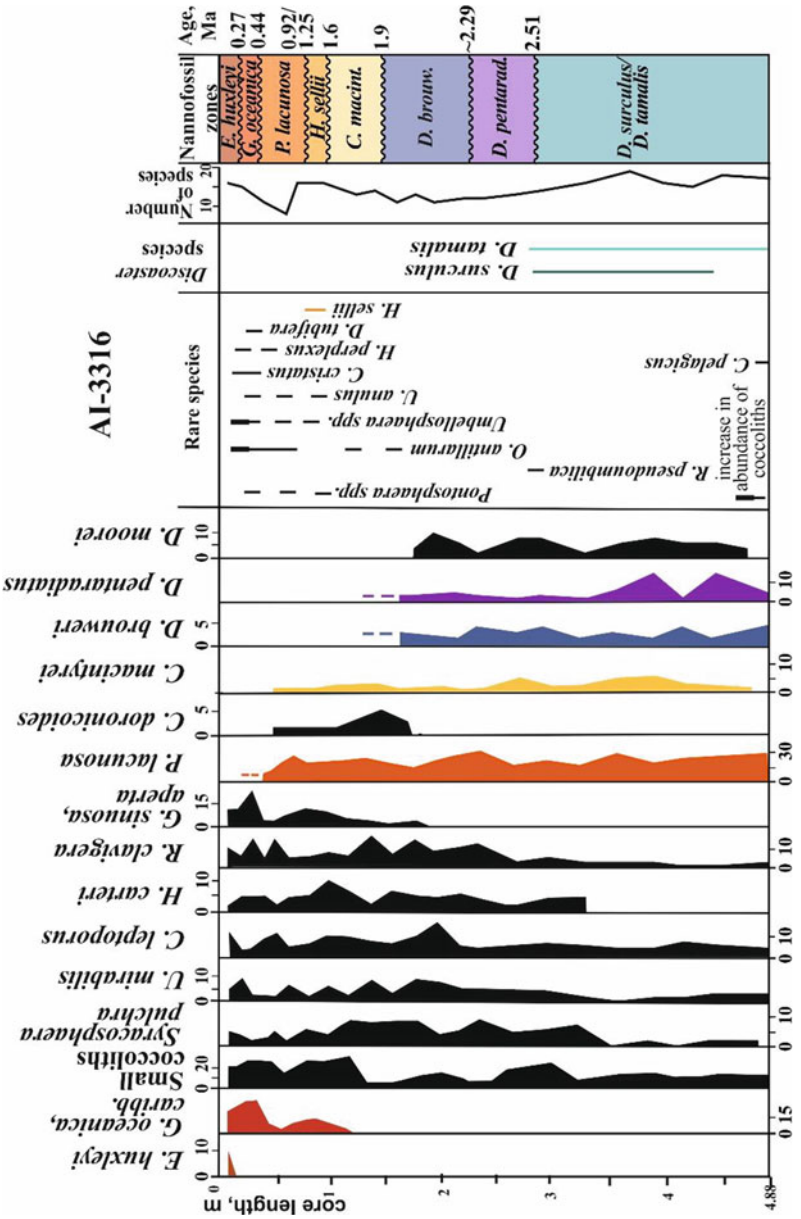

Fig. 9 Down-core distribution of species and nannofossil zones from core AI-3316. See text for the species full names and Fig. 1 for legend

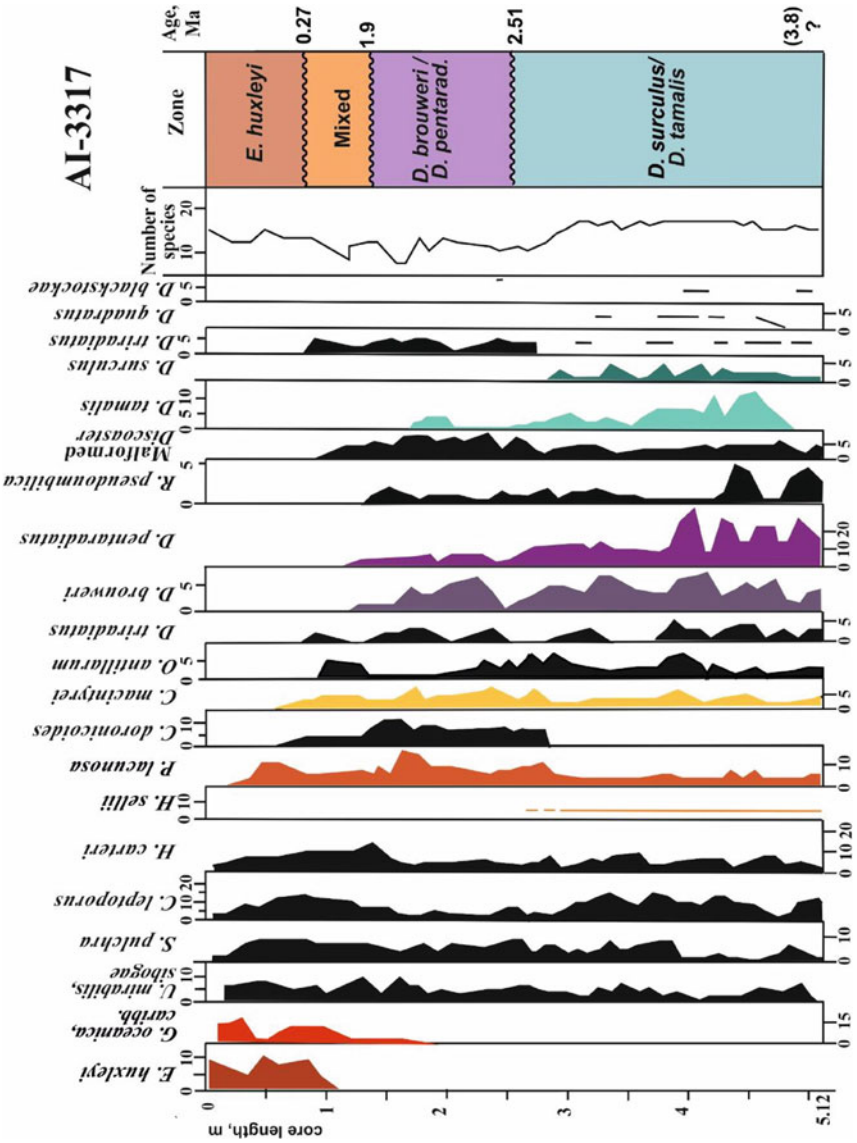

Fig. 10 Down-core distribution of species and nannofossil zones from core AI-3317. See text for the species full names and Fig. 1 for legend

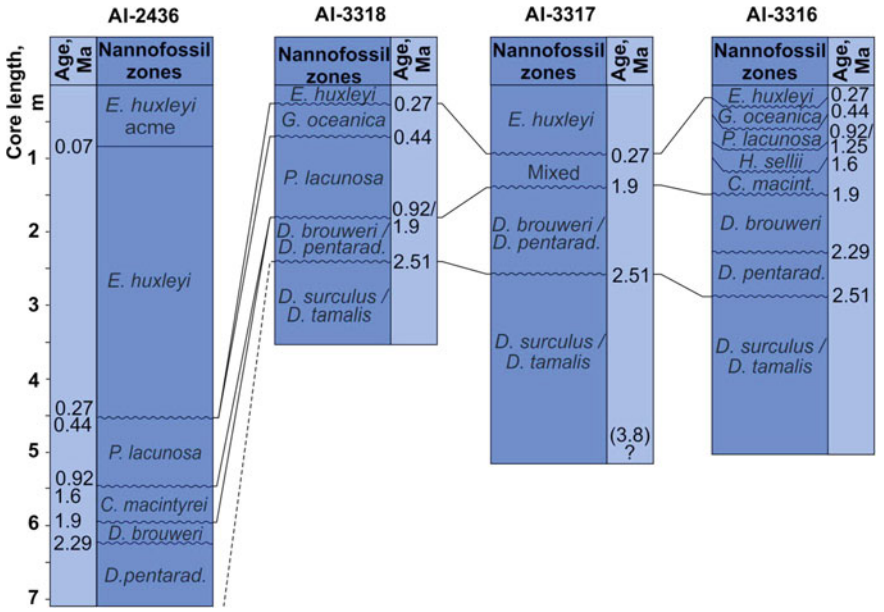

Fig. 11 Correlation of nannofossil zones in four cores studied. See text for the species full names and Fig. 1 for legend

(AI-2436 and AI-3318), some Pleistocene zones are commonly washed out, notably the *Gephyrocapsa oceanica*, the small *Gephyrocapsa*, the *Helicosphaera sellii* and the *Calcidiscus macintyrei* zones. In the Upper Pliocene–Lower Pleistocene sections, the *Discoaster* zones are commonly challenging to differentiate. The thickness of the nannofossil zones also varies with no sustainable trend. We believe that this reflects differences in erosion conditions rather than varying sedimentation rates.

Considering the above data, we conclude that the nannofossil stratigraphy, as well as foraminiferal stratigraphy, suggests widespread hiatuses in the sediment records of the Ioffe Drift area.

4 Correlation of Foraminiferal and Nannofossil Zones in the Ioffe Drift Sediments

In four cores where both microfossil groups were investigated a correlation of the foraminiferal and nannofossil zones seems reasonable, notably on the drift summit (cores AI-2436 and AI-3318) and northern slope (core AI-3316). The shifts in zonal boundaries, probably comprising hiatuses, can be explained by differences in the deposition and reworking of sand-size foraminiferal shells and tiny nannofossils (see Chaps. 6 and 10), and by the evolutional ages of species lineages that are documented

by the FO and LO on the other hand. A good example is presented in Fig. 3 from core AI-3318, where the level of ~1.9 Ma is slightly higher in the nannofossil record than in the foraminiferal record. The longest (0.7–1 Ma) stratigraphic gap from this core is lower in the nannofossil record (0.92/1.9 Ma at ~180 cm, where three zones are absent) than in the foraminiferal record (0.81/1.47 Ma at ~130 cm, where the *Globorotalia crassaformis hessi* zone is absent).

In core AI-3317, with the strongest sediment and microfossil mixing (due to contamination, reworking and erosion), the boundary between foraminiferal zones of *Dentroglobigerina altispira* and *Globorotalia miocenica* at 3.13 Ma corresponds to the younger boundary of the combined *Discoaster tamalis/Discoaster surculus* and *Discoaster pentaradiatus/Discoaster brouweri* zones, at 2.51 Ma. This unexpected coincidence, along with the strong reworking of the fossils in the core section, confirms the occurrence of multiple erosional hiatuses (see also Chap. 9).

No significant increase in the thickness of the biostratigraphic zones or in the number of hiatuses was found between the northern slope (cores AI-3316 and AI-3317) and drift summit area (cores AI-2436, AI-3655 and AI-3318; Fig. 7). The same is true of core AI-3319, collected to the west-southwest of the Ioffe Drift.

5 Correlation of Biostratigraphic Zones from the Ioffe Drift and Rio Grande Rise

The foraminiferal and nannofossil zones in the current study correspond to those previously identified from the Pliocene–Pleistocene section of DSDP Site 516 (Barash et al. 1983; Barash 1988; Dmitrenko 1987); however, they are better represented in the latter section (Fig. 12). This is not surprising, as the foraminiferal preservation is excellent throughout the Pleistocene section of Site 516 (30°16.59′S 35°17.11′W), drilled on the summit of the Rio Grande Rise at a water depth of 1,313 m (Barash et al. 1983), but in the Ioffe Drift sections the preservation is variable.

Although contourite drifts are commonly characterized by high sedimentation rates (e.g., Robinson and McCave 1994; Stow et al. 2013; Rebesco et al. 2014), our previous (Ivanova et al. 2016, 2020) and current findings demonstrate a rather reduced thickness of all recovered upper Pliocene–Quaternary biostratigraphic zones in the sediment sections from the Ioffe Drift area, compared to DSDP Site 516 from the Rio Grande Rise (Ivanova et al. 2016, 2020; Fig. 12). For example, the FO of *Globorotalia truncatulinoides* (1.9 Ma) is identified at 980 cm below sea floor (bsf) at Site 516 (Barash et al. 1983) and at 600 cm in core AI-2436. The only exception, represented by the enhanced thickness of the uppermost zones of *G. ruber* pink and *E. huxleyi* from core AI-2436, resulted from the artificial stretching of the core during processing (Ivanova et al. 2016). Our cores AI-3320 and AI-3321 (see Table 1 in Chap. 4) from the Rio Grande Rise recovered only the uppermost foraminiferal zone of *Globigerinoides ruber* (pink), without any significant foraminiferal reworking. This is in line with the AMS-^{14}C dates suggesting a mean sedimentation rate of

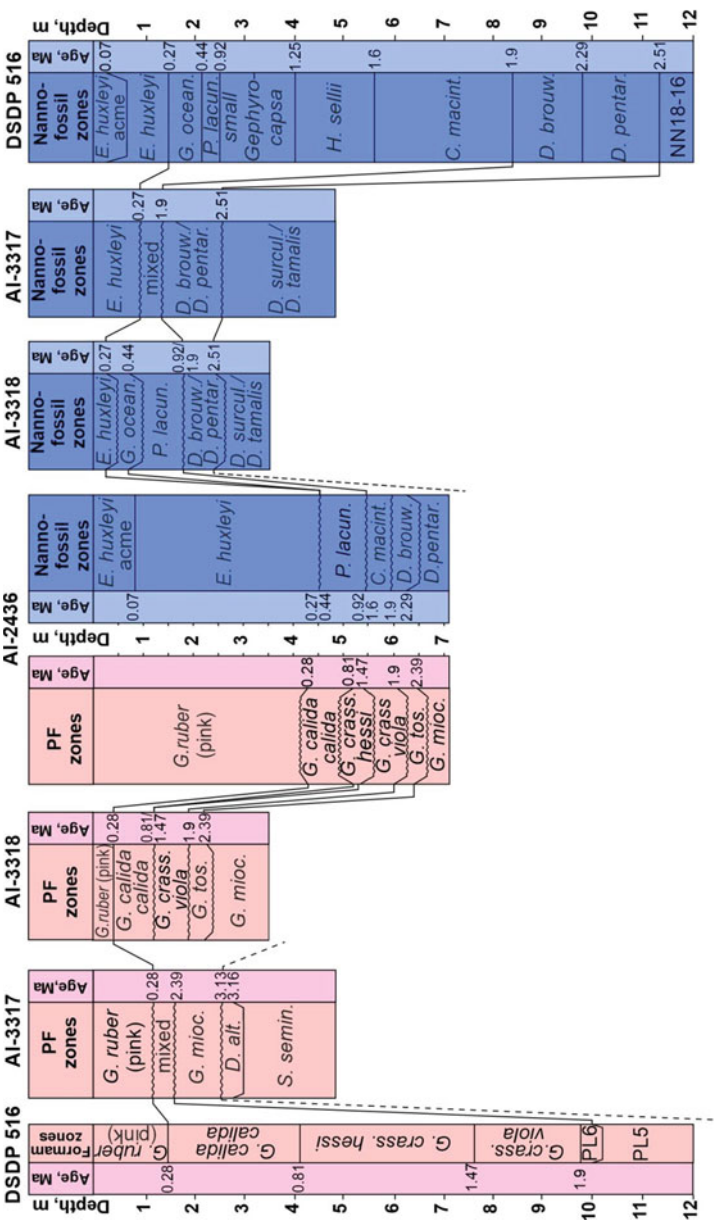

Fig. 12 Correlation of biostratigraphic zones in cores AI-2436 (Ivanova et al. 2016, 2020), AI-3318 (Ivanova et al. 2020), AI-3317, and DSDP Site 516. In the latter, foraminiferal zonation from Barash et al. (1983) and nannofossil zonation from Dmitrenko (1987) are used for the upper ~ 10 m, while the zonation of Berggren et al. (1983a) is applied below (using the zonal boundary ages from Wade et al. (2011) and Bergen et al. (2019). PF zones mean planktic foraminiferal zones. Assumed boundaries between zones and hiatuses are marked by dashed and undulated lines, respectively. See text for the species full names and Fig. 1 for legend

about 0.8 cm/ka for the upper part of both cores AI-3320 and AI-3321 (Table 1). Therefore, these cores support the finding of a greater thickness of biostratigraphic zones at the Rio Grande Rise than at the Ioffe Drift.

The difference in zone thickness in two neighboring areas can be explained first of all in terms of the dominant mechanism of sedimentation. According to Barker et al. (1983), on the Rio Grande Rise, pelagic sedimentation seems to prevail over lateral advection and other mechanisms. As shown in Chap. 6, in the Ioffe Drift the prevailing mechanism of sedimentation comprises lateral advection of biogenic material (originating from pelagic settling) by contour bottom currents. Although pelagic sedimentation is known to be quite slow in oligotrophic areas, the erosional effect of bottom currents in contourites, resulting in hiatuses and stratigraphic gaps, generally overtakes the effect of even relatively fast lateral sedimentation.

Furthermore, we argue that the occurrence of numerous hiatuses explains the aforementioned reduction in the thickness of biostratigraphic zones in the Ioffe Drift area (Ivanova et al. 2020; see also Chap. 9). Any significant impact of selective dissolution on foraminiferal fauna and on the thickness of biostratigraphic zones from the Ioffe Drift cores seems unlikely, apart from in core AI-3319 beyond the drift, from a water depth 4,066 m, and perhaps the lower part of core AI-3317. The aforementioned assumption follows from the generally good, rather good or even perfect preservation of foraminiferal tests in five cores, despite our core sites being much deeper (3,798–3,898 m) than those at DSDP Site 516 (1,313 m). A weak dissolution influence fits well with the established modern 4,050 m-depth of the foraminiferal lysocline in the area (Melguen and Thiede 1974) and probably indicates that during the Late Pliocene–Quaternary the boundary between Lower Circumpolar Deep Water (LCDW) and more corrosive Weddell Sea Deep Water (WSDW) was generally below 3,800 m. The only exception could be some relatively short-term intervals, like during MIS 3–2 for the Vema Channel area, as shown in Ovsepyan and Ivanova (2019).

If the identified hiatuses are of erosional origin, it means that surface bioproductivity and pelagic sedimentation in the Ioffe Drift area were not necessarily slower than at similar depths in the subtropical South Atlantic, where the thickness of Upper Pliocene–Quaternary sections is commonly greater than in our cores (Fig. 12; see also Chap. 9). Rather, the sediments were washed out by post-depositional erosion.

6 Conclusions

The sediment cores collected from the Ioffe Drift area recovered Upper Pliocene–Quaternary sediments. The biostratigraphic study of six sediment cores from the area permitted the identification of the eight foraminiferal and nine nannofossil (in four cores) zones described in Ivanova et al. (2016, 2020) and in Chap. 3. Core AI-3317, from the northern slope, spanned presumably the last ~4 Ma; that is, it penetrated deeper into the Upper Pliocene sediments than the other five cores.

The suggested foraminiferal and nannoplankton zonations collectively provide a robust stratigraphic framework for a multi-proxy study of the Ioffe Drift sediments and for paleoceanographic inferences.

The foraminiferal stratigraphic zonation developed for the six cores and visual estimates of the shells preservation collectively suggest that the drift slopes, unlike the summit, were affected by selective dissolution, notably in the late Pliocene. The strongest dissolution impact on foraminiferal fauna is documented from the lower half (i.e., in the Lower Pleistocene section) of core AI-3319, collected to the west-southwest of the Ioffe Drift.

The thickness of all biostratigraphic zones in the Ioffe Drift sections is significantly less than those in DSDP Site 516 on the nearby Rio Grande Rise. Nannofossil zones, notably those of *Gephyrocapsa oceanica*, *Helicosphaera sellii*, *Calcidiscus macintyrei*, *Pseudoemiliania lacunosa,* and especially of small *Gephyrocapsa*, are commonly washed out, like the foraminiferal zone of *Globorotalia crassaformis hessi*. In core AI-3317, the latter is mixed with the *Globigerinella calida calida, Globorotalia crassaformis viola* and *Globorotalia tosaensis* zones.

The reduced thickness and/or absence of foraminiferal and nannofossil zones, resulting in stratigraphic gaps in the sediments from the Ioffe Drift area, suggests the occurrence of several erosion hiatuses, as discussed in Chap. 9.

References

Backman J, Raffi I, Rio D et al (2012) Biozonation and biochronology of Miocene through Pleistocene calcareous nannofossils from low and middle latitudes. Newsl Stratigr 45:221–244. https://doi.org/10.1127/0078-0421/2012/0022

Barash MS, Oskina NS, Bylum NS (1983) Quaternary biostratigraphy and surface paleotemperatures based on planktonic foraminifers. In: Barker PF, Johnson DA, Carlson RL (eds) Initial reports of the deep-sea drilling project, 72. Government Printing Office, Washington, U.S, pp 849–869

Barash MS (1988) Quaternary paleooceanology of the Atlantic Ocean. Nauka (in Russian), Moscow

Barker PF, Johnson DA, Carlson RL et al (1983) Site 516: Rio Grande Rise. In: Barker PF, Johnson DA, Carlson RL (eds) Initial Reports of the deep-sea drilling project, 72. Government Printing Office, Washington, U.S, pp 155–338

Bergen JA, Truax S, de Kaenel E et al (2019) BP Gulf of Mexico Neogene astronomically-tuned time scale (BP GNATTS). Bull Geol Soc Am 131:1871–1888. https://doi.org/10.1130/B35062.1

Berggren WA, Aubry MP, Hamilton N (1983) Neogene magnetobiostratigraphy of deep-sea drilling project, site 516: Rio Grande Rise, South Atlantic. In: Barker PF, Carlson RL, Johnson DA (eds) Initial reports of deep-sea drilling project 72. Government Printing Office, Washington, U.S, pp 675–713

Berggren WA, Hamilton N, Johnson DA, Pujol C, Weiss W, Cepek P, Gombos AM Jr (1983) Magnetobiostratigraphy of deep-sea drilling project 72, sites 515–518: Rio Grande Rise (South Atlantic). In: Barker PF, Carlson RL, Johnson DA (eds) Initial reports of deep-sea drilling project 72. Government Printing Office, Washington, U.S, pp 939–948

Berggren WA, Hilgen FJ, Langereis CG et al (1995) Late Neogene chronology: new perspectives in high-resolution stratigraphy. Geol Soc Am Bull 107:1272–1287. https://doi.org/10.1130/0016-7606(1995)107%3c1272:LNCNPI%3e2.3.CO;2

Blow WH (1969) Late Middle Eocene to recent planktonic foraminiferal biostratigraphy. In: Brönnimann P, Renz HH (eds) Proceedings of the first international conference on planktonic microfossils, 1st edn. EJ Brill, Leiden, Geneva, pp 199–422

Bolli HM, Saunders JB (1985) Oligocene to Holocene low latitude planktonic foraminifera. In: Plankton Stratigraphy. Cambridge University Press, pp 155–262

Dmitrenko OB (1987) A detailed zonal scale of the quaternary bottom deposits based on coccoliths (on the Rio Grande rise in the Atlantic ocean). Oceanology 27(3):460–464 (in Russian with English translation)

Gartner S (1977) Calcareous nannofossil stratigraphy and revised zonation of the Pleistocene. Mar Micropal 2:1–25

Ivanova E, Murdmaa I, Borisov D et al (2016) Late Pliocene-Pleistocene stratigraphy and history of formation of the Ioffe calcareous contourite drift, Western South Atlantic. Mar Geol 372:17–30. https://doi.org/10.1016/j.margeo.2015.12.002

Ivanova E, Borisov D, Dmitrenko O, Murdmaa I (2020) Hiatuses in the late Pliocene-Pleistocene stratigraphy of the Ioffe calcareous contourite drift, western South Atlantic. Mar Pet Geol 111:624–637. https://doi.org/10.1016/j.marpetgeo.2019.08.031

Kennett JP, Srinivasan MS (1983) Neogene Planktonic Foraminifera: a phylogenetic atlas. Hutchinson Ross Publishing Company, Stroudsburg, Pensilvania

Melguen M, Thiede J (1974) Facies distribution and dissolution depths of surface sediment components from the Vema channel and the Rio Grande Rise (southwest Atlantic Ocean). Mar Geol 17:341–353. https://doi.org/10.1016/0025-3227(74)90096-6

Ovsepyan EA, Ivanov EV (2019) Glacial–interglacial interplay of southern- and northern-origin deep waters in the São Paulo Plateau-Vema channel area of the western South Atlantic. Palaeogeogr Palaeoclimatol Palaeoecol 514:349–360. https://doi.org/10.1016/j.palaeo.2018.10.031

Rahman A, Roth PH (1989) Late Neogene calcareous nannofossil biostratigraphy of the Gulf of Aden region. Mar Micropaleontol 15:1–27. https://doi.org/10.1016/0377-8398(89)90002-9

Rebesco M, Hernández-Molina FJ, Van Rooij D, Wåhlin A (2014) Contourites and associated sediments controlled by deep-water circulation processes: state-of-the-art and future considerations. Mar Geol 352:111–154. https://doi.org/10.1016/j.margeo.2014.03.011

Robinson SG, McCave IN (1994) Orbital forcing of bottom-current enhanced sedimentation on Feni drift, NE Atlantic, during the mid-Pleistocene. Paleoceanography 9:943–972. https://doi.org/10.1029/94PA01439

Schiebel R, Hemleben C (2017) Planktic foraminifers in the modern ocean. Springer, Berlin

Stow DAV, Hernandez-Molina FJ, Alvarez-Zarikian CA (2013) Expedition 339 Scientists (2013) Expedition 339 summary. In: Stow DAV, Hernández-Molina FJ, Alvarez Zarikian CA, Expedition 339 Scientists (eds) Proceedings of the IODP, 339. Integrated Ocean Drilling Program Management International, Inc., Tokyo. https://doi.org/10.2204/iodp.proc.339.101.2013

Wade BS, Pearson PN, Berggren WA, Pälike H (2011) Review and revision of Cenozoic tropical planktonic foraminiferal biostratigraphy and calibration to the geomagnetic polarity and astronomical time scale. Earth-Science Rev 104:111–142. https://doi.org/10.1016/j.earscirev.2010.09.003